A member of wheat class III peroxidase gene family, *TaPRX-2A*, enhanced the tolerance of salt stress

Peisen Su
Shandong Agricultural University
Jun Yan
Shandong Agricultural University
Wen Li
Shandong Agricultural University
Liang Wang
Shandong Agricultural University
Jinxiao Zhao
Shandong Agricultural University
Xin Ma
Shandong Agricultural University
Anfei Li
Shandong Agricultural University
Hongwei Wang
Shandong Agricultural University
Lingrang Kong (lkong@sdau.edu.cn)
Shandong Agricultural University

Research article

Keywords: Wheat, Salinity stresses, Peroxidases, TaPRX-2A

Posted Date: May 11th, 2020

DOI: https://doi.org/10.21203/rs.2.20974/v2

Version of Record: A version of this preprint was published at BMC Plant Biology on August 26th, 2020.
See the published version at https://doi.org/10.1186/s12870-020-02602-1.

Abstract

Background: Salt and drought are the main abiotic stresses that restrict yield of crops. It is reported that peroxidases (PRXs) are involved in various abiotic stress responses. However, few wheat PRXs are characterized in the mechanism of abiotic stresses.

Results: In this study, a novel wheat peroxidase (PRX) gene named TaPRX-2A, a member of wheat class III peroxidase gene family, was cloned and characterized in salt stress response. Based on the identification and evolutionary analysis of class III PRXs in 12 plants, we proposed an evolutionary model that TaPRX-2A might have experienced some exon fusion events during evolution. We also detected the positive selection of PRX domain in 13 PRXs involving our evolutionary model, and found 2 or 6 positively selected sites during TaPRX-2A evolution. The results of expression pattern showed that TaPRX-2A exhibited relatively higher expression levels in root tissue compared with that of leaf and stem tissues by using qRT-PCR. This TaPRX-2A was also induced by some stresses and hormone treatments including PEG6000, NaCl, hydrogen peroxide (H 2 O 2), salicylic acid (SA), methyljasmonic acid (MeJA) and abscisic acid (ABA). Transgenic wheat plants with overexpression of TaPRX-2A showed higher tolerance to salt stress than wild type (WT) plants. Confocal microscopy revealed that TaPRX-2A :eGFP was mainly localized in nuclei. The survival rate, relative water content and shoot length were higher in TaPRX-2A -overexpressing wheat than WT. However, root lengths were no significant difference between transgenic wheat and WT. The activities of superoxide dismutase (SOD), peroxidase (POD), and catalase (CAT) were enhanced in TaPRX-2A -overexpressing wheat than WT, resulting in the reduction of reactive oxygen species (ROS) accumulation and malondialdehyde (MDA) content. We also measured the expression levels of downstream stress-related genes (RD22 , TLP4 , ABAI , GLP4 , GST22 , FeSOD, CuSOD, and CAT). The results showed that RD22 , TLP4 , ABAI , GST22 , FeSOD, and CAT exhibited higher expression in TaPRX-2A -overexpressing lines than in WT under salt stress.

Conclusions: The results show that TaPRX-2A plays a positive factor in response to salt stress by scavenging ROS and regulating stress-related genes.

Background

Abiotic stresses such as high salinity and drought have profound negative impacts on plant development and biomass formation, resulting in significant reductions in crop yield worldwide [1]. In order to adapt to abiotic stresses, plants have evolved complex mechanisms for physiological and biochemical mitigation of stress-associated damage, such as release of reactive oxygen species (ROS) [2,3]. Previous studies have shown that hydrogen peroxide (H_2O_2) pretreatment can improve the salt tolerance of wheat by modulating the activity of antioxidant enzymes, mineral uptake, and proline levels [4]. In the cells of higher plant, reactive oxygen species (ROS) exist in many forms, including hydrogen peroxide (H_2O_2), superoxide radicals ($O_2^{\cdot-}$) and hydroxyl radicals (OH^-). ROS are generated under abiotic conditions and cause rapid cell damage by damaging membrane lipids, nucleic acids and so on [5]. Plants have established a complex system to scavenge ROS for maintaining the steady-state level of ROS by

activating the antioxidant system. The antioxidant system refers mainly to free-radical scavenging by several endogenous antioxidant enzymes, including glutathione peroxidase (GPX), ascorbate peroxidase (APX), catalase (CAT) and superoxide dismutase (SOD) [6,7,8]. It has been reported that antioxidant enzymes (APX, CAT) are also altered when plants were in salt stress [3,9,10]. In addition, peroxidases (PRXs) have been reported to protect cells against ROS by catalyzing oxidoreduction [11].

PRXs exist in many species, such as microorganisms, animals and plants [12,13,14,15]. PRXs are divided into three superfamilies based on different structures and catalytic properties. The first PRXs superfamily includes animal enzymes including eosinophill peroxidase and glutathione peroxidase. The second PRXs superfamily is widely distributed in many species (bacteria, animals, fungi, plants, and yeast). The third PRXs superfamily has functions in plants, bacteria and fungi [14,15]. According to differences in primary structure, PRXs are divided into three classes, including class I PRXs distributed in intracellular, class II PRXs distributed in extracellular and class III PRXs comprised large multigene families [16]. Class I PRXs play key roles in scavenging excess H_2O_2 [16,17,18]. Class II PRXs are from fungi involved in the degradation of soil debris [16,19]. In many plants, plant-specific PRXs belong to class III PRXs [20]. More than 110 class III PRXs have been found in allohexaploid wheat [21]. *Oryza sativa* comprises 138 class III PRXs [22]. Seventy-three sequences encode class III PRXs of *Arabidopsis thaliana,* and 119 class III PRXs have been identified in maize [12,23]. *Populus trichocarpa* contains 93 class III PRXs [24].

Class III PRXs play various functions in plant development processes, including cell wall hardening, crosslinking of cell wall components, defense against pathogen infection, H_2O_2 removal and wounding [12,16,25]. In *A. thaliana*, a large number of PRXs have been studied and proved the function. For example, *AtPRX72* plays an important role in lignification [26]. *AtPRX33* and *AtPRX34* were identified to play a function in cell elongation [16]. Some studies have demonstrated that *AtPRX21, AtPRX62* and *AtPRX71* are response to wounding and fungal stresses [27,28]. *Gossypium hirsutum* gene *GhPOX1* may cause cotton fiber cell elongation through reactive oxygen species production [29]. Some PRXs have been reported that play a central role in host plant defenses against necrotrophic or biotrophic pathogens by coordinating salicylic acid (SA), jasmonic acid (MeJA), or ethylene (ET) [20]. For example, *TaPRX111, TaPRX112* and *TaPRX113* are involved in plant response to nematode infection in wheat [30]. In rice, expression patterns of the 21 PRXs are revealed important diversity, especially in response to stresses [31]. The *Zea mays* PRXs, *ZmPRX26, -42, -71, -75* and *-78* are respond to various abiotic stress conditions [12]. In addition, glutathione peroxidases (GPXs) are members of peroxidases family and play an important function in plant. The *A. thaliana* GPX gene, *AtGPX3,* acts as a general scavenger and signal transducer under drought stress and ABA signaling [32]. Six *CsGPXs* (*Cucumis sativus*) are identified to respond to ABA treatments and abiotic stress. Moreover, 5 rice GPXs are identified to play a role in H_2O_2 and cold stress [33]. Several wheat PRXs have been discovered to function in drought-resistant by a microarray experiment [34]. Two wheat GPXs, W69 and W106 have been showed to improve the salt tolerance in transgenic *Arabidopsis* [7].

Wheat is an important crop in the world, and its yield is often constrained by abiotic stresses [35,36]. The roles of some PRXs in salt stress tolerance have been reported before. However, the molecular

mechanisms of PRXs in salt response are still not fully understood in wheat. In this report, we cloned a peroxidase gene *TaPRX-2A* from wheat (*Triticum aestivum*). Evolutionary analysis revealed that some exon fusion events and positive selection might have happened during *TaPRX-2A* evolution. Gene expression pattern analysis demonstrated that *TaPRX-2A* was up-regulated by drought, salt, H_2O_2 and ABA treatments. We further investigated the salt stress tolerance conferred by *TaPRX-2A* in transgenic wheat. Ultimately, our results showed that *TaPRX-2A* improved the wheat salt tolerance by improving antioxidative stress ability and regulating stress-related genes. Our work will give the researchers new insights into the mechanisms underlying *TaPRX-2A* function in abiotic stress tolerance.

Results

Isolation and evolution of *TaPRX-2A*

In order to obtain further insights into evolutionary conservation or divergence among class III peroxidases (PRXs), we performed identification, classification and gene structures of class III PRXs. PRXs of 12 plants (*T. aestivum*, *Triticum dicoccoides*, *Triticum urartu*, *Aegilops tauschii*, *Brachypodium distachyon*, *O. sativa*, *Z. mays*, *A. thaliana*, *Vitis vinifera*, *Selaginella moellendorffii, Physcomitrella patens* and *Chlamydomonas reinhardtii*) were identified by HMMER 3.1 and Pfam 32.0 in batch mode with the PRX domain (peroxidase.hmm, PF00141.23) (Additional file 1: Table S1, and Additional file 2: Table S2). We excluded the atypical PRXs of these 12 plants with less than 50% alignment of PRX domain in the following analysis (Additional file 3: Table S3). The classification of these PRXs was based on two methods, HMMER3.1 scan and neighbour-joining (NJ) phylogenetic reconstruction (Additional file 2: Table S2 and Additional file 4: Figure S1). The exon-intron structures within the PRXs domain were also diagrammed in 12 investigated plants (Additional file 5: Figure S2).

Among them, we cloned one member (named *TaPRX-2A*) of the PRXs in the wheat cultivar “Sumai 3”. The predicted *TaPRX-2A* ORF is 1026 bp, and the deduced *TaPRX-2A* protein comprises 342 amino acid residues. BLAST results at NCBI showed that a PRX gene (GenBank: AJ878510.1) in *T. aestivum* cultivar “Cheyenne” contained the minimum E value. Our local BLAST against identified PRXs of 12 plants showed that one *T. aestivum* PRX (TraesCS2A02G573900.1.cds1) from subfamily VI contained 100% sequence similarity with *TaPRX-2A.* In order to investigate the evolution of this clone, we reconstructed a small NJ phylogenetic tree only containing subfamily VI PRXs from 12 plants, and compared their structural features (Fig. 1a-b). As shown, the exon-intron structure of this *T. aestivum* clone (TraesCS2A02G573900.1.cds1) was one-exon structure, while the other four wheat and *Ae. tauschii* homologous PRXs (Tdi_TRIDC2AG080470.2, Ata_AET2Gv21275100.1, Tae_TraesCS2B02G613900.1.cds1, Tdi_TRIDC2BG088710.2) in this clade were also one-exon structure, suggesting that this one-exon structure might have originated in these PRXs before the *Triticum-Aegilops* split (Fig. 1b).

Based on the phylogenetic and exon-intron structure analysis (Additional file 5: Figure S2), we proposed an evolutionary model to infer the origin of *TaPRX*-2A (TraesCS2A02G573900.1.cds1), which was

involved in the processes of exon fusion (Fig. 2a). Moreover, we concluded that two rounds of exon fusion events occurred during the Angiosperm and *Gramineae* emergence. The first exon fusion event (4 exons changed into 3 exons) occurred during the Angiosperm emergence. An ancestral sequence resembling *P. patens* PRX (Pp3c19_20780V3.3) contained a conserved exon-intron structure within four exons and the “001” exon phases near PRX domain. This four-exon structures within “001” exon phases retained in the ancestral sequences resembling two *S. moellendorffii* PRXs (Smo_EFJ32905 and Smo_EFJ15769). However, the exon-intron structures of PRXs in *A. thaliana* (Ath_AT1G71695.1)*, V. vinifera* (Vvi_VIT_18s0072g00160.t01) and *O. sativa* (Osa_Os04t0688200–01) changed into the three-exons within “00” exon phases, suggesting that a exon fusion event might have happened in the last two exons of four-exon structures within “001” exon phases before the monocot-eudicot split. The second exon fusion event (3 exons changed into 2 exons or 1 exon) occurred during the *Gramineae* emergence. As shown in Fig. 2a, the first two exons in three-exon structure within “00” exon phases could have fused, and changed into the two-exon structure within “0” exon phase (*B. distachyon*, KQJ85452). Similarly, the last two exons could have also fused (*T. aestivum,* TraesCS2A02G574400.1; *T. urartu,* TRIUR3_03591-P1). Even all of the three exons could have fused, and became into a single exon structrure (*Ae. Tauschii,* Ata_AET2Gv21275100.1; *T. dicoccoides,* Tdi_TRIDC2AG080470.2, Tdi_TRIDC2BG088710.2; *T. aestivum,* TraesCS2A02G573900.1.cds1, Tae_TraesCS2B02G613900.1.cds1). The alignments of these PRXs within the breakpoints of exon fusion events supported our evolutionary model (Fig. 2b).

In order to confirm these PRX sequences for *TaPRX-2A* evolutionary model, we checked them for cDNA-level evidences in RNA-seq data from seven plants, including *P. patens*, *A. thaliana*, *V. vinifera*, *B. distachyon*, *Ae. tauschii*, *T. dicoccoides* and *T. aestivum* (Additional file 6: Table S4). We did not detected them in *S. moellendorffii* and *T. urartu* because their GFF3 annotation files were just in scaffolds, not in chromosomes. The results showed that most of the PRX sequences (except VIT_18s0072g00160.t01 and TraesCS2A02G574400.1) from seven plants were detected in RNA-seq data (FPKM and coverage values in “information” column of Additional file 6: Table S4), hinting that *TaPRX-2A* evolution model of exon fusion may happen during the plant evolution.

We also detected positive selection of PRX domain sequences in *TaPRX-2A* and other 12 homologous PRXs by using PAML 4.9 (Table 1). According to the LRT (likelihood ratio test) of site-specific models, model M2a (selection) was more significantly higher than M1a (neutral) ($df=2$, $2\Delta lnL=68.4$, $P<0.005$), indicating that some amino acid sites underwent positive selection during evolution. The M7-M8 comparison ($df=2$, $2\Delta lnL=7.47$, $P<0.025$) also supported the assertion of positive selection. These positively selected sites were found by using Naive Empirical Bayes (NEB) and Bayes Empirical Bayes (BEB) analysis (Additional file 7: Figure S3a,b). Two (95 E and 185 K, refer to sequence: Smo_EFJ32905) and six positively selected sites (95 E, 110 S, 117 Q, 135 E, 185 K and 212 R) were found in M2a and M8 model, respectively. Ancestral sequences in evolutionary nodes were also inferred by PAML 4.9 and MEGAX (Additional file 7: Figure S3).

Expression patterns of *TaPRX-2A* in various tissues and stress treatments

To detect the expression patterns of *TaPRX-2A* in response to stress-related signaling, we performed qRT-PCR in different tissues (leaf, stem, and root) and with different stress treatments (PEG6000, NaCl, H_2O_2, SA, MeJA, IAA, and ABA). The results showed that *TaPRX-2A* was differentially expressed in roots, stems and leaves, with significantly higher expression levels in root tissue compared with that of leaf and stem tissues (Fig. 3a). Then, we checked the expression patterns of *TaPRX-2A* by using qRT-PCR in treatments of PEG6000, NaCl and H_2O_2. The results showed that the expressions of *TaPRX-2A* were induced by PEG6000, NaCl and H_2O_2 treatments, and the expression levels reached a perk at 6 h (hour) after treatments (Fig. 3b,c and d). We also examined the expression patterns in treatments of four phytohormones. As shown in Fig. 3e, *TaPRX-2A* exhibited approximately 2.5-fold upregulation at 1 h after SA treatment (Fig. 3e). Similarly, the expression levels of *TaPRX-2A* reached a peak at 6 h after JA and ABA treatments (Fig. 3f, h). However, the expression levels of *TaPRX-2A* remained relatively unchanged throughout 0-6 h after IAA treatment, but exhibited an approximate 1.5-fold up-regulation at 12 h (Fig. 3g). These results showed that this *TaPRX-2A* was involved in various abiotic stress responses.

Subcellular localization of the *TaPRX-2A* protein

To characterize the function of *TaPRX-2A*, the ORF of *TaPRX-2A* was fused to a pBIN35S-eGFP vector under the control of a CaMV 35S promoter (Additional file 8: Fig. S4a). The pBIN35S:eGFP empty vector control and the pBIN35S:*TaPRX-2A*:eGFP recombinant vector construct were transformed into tobacco leaf cells by *Agrobacterium* infiltration. We observed the epidermal cells of injected *N. benthamiana* leaves by confocal microscopy, and found that *TaPRX-2A*:eGFP was mainly localized in nuclei (Additional file 8: Fig. S4b_1-d_2). In addition, the pBIN35S-*TaPRX-2A*-eGFP and pBIN*35S*-eGFP vector were transformed into onion epidermal cells. Consistent with the localization results observed in tobacco epidermal cells, the *TaPRX-2A*:eGFP was also mainly localized in nuclei of the onion epidermal cells (Additional file 8: Fig. S4b_3-d_4). Moreover, the prediction of web server cNLS showed that five NLSs (nuclear localization signals) sequences existed in *TaPRX-2A* (Additional file 9: Figure S5).

TaPRX-2A enhanced the salt tolerance in transgenic wheat

To further confirm the function of *TaPRX-2A* in salt stress responses, we transformed wheat cultivar “KN199” with a *TaPRX-2A*-overexpression and constructed three independent transgenic lines (TaOE1, TaOE2 and TaOE3). The expression profile of *TaPRX-2A* was analyzed in *TaPRX-2A* transgenic lines through qRT-PCR. The results showed that transgenic lines exhibited higher expression level than wild type (WT) plants (Additional file 10: Fig. S6a). Then, we measured the peroxidase activity in three independent transgenic lines and WT. The peroxidase activity was higher in transgenic lines than WT

(Additional file 10: Fig. S6b). Taken together, we concluded that *TaPRX-2A* overexpression caused high peroxidase activity in transgenic lines.

Then, we measured the phenotypic differences between transgenic lines (three independent lines, TaOE1, TaOE2 and TaOE3) and WT in salt stress conditions. Under non-stress condition, no visibly phenotypic difference was observed between TaOE1-3 and WT. Under salt condition, the TaOE lines showed stronger growth comparing with the WT. In addition, the WT leaves turned yellow and wilted under salt stress, while the TaOE leaves still remained green (Fig. 4a). We also found that the survival rate of WT plants was only 40% after salt treatment, whereas the survival rates among TaOE1, TaOE2, and TaOE3 plants were 63.6%, 57.6%, and 63%, respectively (Fig. 4b). We then compared the shoot lengths, relative water content (RWC), and root lengths between WT and TaOE plants under salt treatment (Fig. 4c, d and e). The results showed that transgenic lines exhibited longer shoot length and higher RWC than WT plants. However, no significant difference in root lengths was observed between WT and transgenic lines. Taken together, these results indicated that *TaPRX-2A* overexpression dramatically enhanced the salt tolerance in wheat.

To further explore mechanisms underlying *TaPRX-2A*-mediated response to salt stress response, we measured physiological-biochemical indices between TaOE and WT plants under non-stress and salt stress conditions (Fig. 5a-d). Under salt treatment, TaOE lines contained significantly lower malondialdehyde (MDA) content than WT, but higher soluble sugar, proline, and soluble protein contents. Moreover, the proline contents of transgenic lines were approximately 2-fold greater than that of WT (Fig. 5c). These results suggested that overexpression of *TaPRX-2A* increased the contents of metabolites which were necessary for osmotic and oxidative stress tolerance in wheat cultivars “KN199”, thus resulting in improving tolerance to salt.

TaPRX-2A regulates ROS scavenging and the expression of stress-related genes in transgenic wheat

Previous studies showed that the tolerance to oxidative stress was associated with plant physiological response to abiotic stresses [35,55,56]. We therefore examined the function of *TaPRX-2A* in reducing ROS levels in transgenic lines under salt stress. As major indicators of the ROS level, we assayed the accumulation of O_2^- and H_2O_2 for comparison between TaOE and WT lines using Nitroblue Tetrazolium (NBT) and 3-diaminobenzidine (DAB) staining. Under salt treatment, we found that levels of O_2^- (stained blue with NBT) and H_2O_2 (stained brown by DAB) were significantly lower in TaOE transgenic lines than in WT (Fig. 6a-d). In addition, the activities of superoxide dismutase (SOD), peroxidase (POD), and catalase (CAT) antioxidant enzymes were also measured between TaOE and WT plants. The results indicated that the transgenic plants contained higher activities of SOD, CAT and POD antioxidant enzymes than the WT plants (Fig. 6e-g).

To determine whether stress-responsive genes were associated with enhancing the salt tolerance by *TaPRX-2A*, We checked the expression patterns of various stress-related genes in TaOE plants by using qRT-PCR (Fig. 7). These stress-related genes (encoding dehydration-responsive protein, *RD22*; thaumatin-like protein, *TLP4*; ABA-inducing, *ABAI*; germin-like protein, *GLP4*; glutathione S-transferase, *GST22*; and the genes encoding ROS-scavenging enzymes *FeSOD, CuSOD,* and *CAT*) were reported to be response to various abotic stresses. The results showed that majority of these stress-related genes had higher expression in TaOE lines than in WT under salt stress. However, expression of *CuSOD* was not significantly different between WT and transgenic lines under salinity stress. In addition, we found lower expression of some stress-related genes in WT plants under non-stress conditions, including *RD22, ABAI,* and *CAT.* Taken together, these results indicated that *TaPRX-2A* overexpression may improve salt tolerance in wheat by enhancing the transcription levels of stress-responsive genes.

Discussion

The evolution of *T. aestivum TaPRX-2A*

The objective of this work is to characterize the role of the wheat peroxidase gene *TaPRX-2A* response to salt stress, in light of the severe reduction in crop yields associated with this abiotic stress [57]. Based on the classification of NJ phylogenetic tree and HMM scan, TraesCS2A02G573900.1.cds1 belongs to subfamily VI PRXs. Subfamily VI PRXs can be found in *S. moellendorffii*, but not in *P. patens*, suggesting that subfamily VI PRXs might have appeared in fern-resembling ancestors. Subfamily VI PRXs contain only one member in two investigated eudicots (*A. thaliana* and *V. vinifera*). While subfamily VI PRXs contain various members in investigated monocots (Additional file 5: Figure S2), suggesting that subfamily VI might have experienced monocot-specific duplication events after monocot-eudicot split.

Based on the analysis of exon-intron diagrams of 12 investigated plants, we proposed an evolutionary model involving two rounds of exon fusion events to infer the origin of *TaPRX*-2A (TraesCS2A02G573900.1.cds1) (Fig. 2). Among these exon fusion events, we focused on one of the second round exon fusion event, that three-exon structure chaged into one-exon structure before the *Triticum-Aegilops* split (formed into *TaPRX*-2A ancestor). The possible mechanism of this one-exon structure emergence might be “retroposition” (the newly duplicated paralogs lack introns, as a result of retrotransposition), which was reported in the origin of gene *jingwei* in *Drosophila* species [58], and ATP synthase PGAM3 [59]. For instance, PGAM1 contains three introns, while PGAM3 is intron-less. In plants, 69 retroposons and 1235 primary retrogenes were identified in *A. thaliana* and *O. sativa*, respectively [60,61]. We also detected the positive selection among these 13 PRXs of evolutionary model by PAML4.9, and found 2 or 6 positively selected sites. It was also reported that 7 gene pairs among 24 retrogenes in *Oryza* species were identified to be under positive selection [62].

TaPRX-2A enhanced the antioxidative stress ability, resulting in improving the salt tolerance in wheat

In higher plants, class III PRXs comprise a large gene family, the members of which have been reported to participate in plant response to abiotic stress [16]. For example, *O. sativa* class III PRXs gene *OsPRX38* were reported to improve *Arabidopsis* arsenic (As) tolerance by activating the antioxidant system (SOD, PRX, GST) and scavenging H_2O_2 [63]. In tobacco, it has been showed that overexpression of a class III PRX gene (*AtPrx64*) of *A. thaliana* improved the plant's aluminum tolerance by increasing the root growth and scavenging accumulation of aluminum and ROS [64]. In *A. thaliana,* overexpression of *AtPRX3* was shown to improve the dehydration and salt tolerance. However, inhibition of *AtPRX3* expression decreased the tolerance to dehydration and salt [65]. In addition, the *Catharanthus roseus* class III peroxidases, *CrPrx1* and *CrPrx* have been reported to improved germination rate under salt stress in *Nicotiana tabacum* [66]. Consistent with these reports, our results also proved a positive regulator in salt tolerance of wheat by *TaPRX-2A.*

Among the physiological issues that accompany abiotic stress in plants, accumulation of excessive ROS, particularly O_2^-, H_2O_2 and high concentrations of ROS, can damage cell membrane permeability, integrity, and cell compartmentation [41,67,68,69]. Plant class III PRXs can catalyze hydrogen peroxide (H_2O_2) reduction in peroxidative cycle by transferring electrons from different donors [13,16]. Previous studies have shown that class III PRXs can improve stress tolerance by regulating the ROS balance in plants. For example, *OsPRX38* improve *Arabidopsis* arsenic (As) tolerance by activating the antioxidant system and scavenging H_2O_2 [63]. *AtPrx64* improves plant's aluminum tolerance by scavenging accumulation of ROS [64]. To maintain ROS balance through scavenging of free radicals, plants have evolved a complex antioxidative system to protect cells from damage [67,69]. Notably, SOD, CAT and POD enzymes expression reportedly contributes to enhanced salt tolerance [9,10]. In our study, we found that *TaPRX-2A* overexpression improved antioxidant activity by CAT and POD enzymes, thereby reducing ROS levels. In addition, the expression of antioxidant genes *FeSOD, CuSOD,* and *CAT* was altered in the *TaPRX-2A* overexpression transgenic plants comparing with WT, suggesting that *TaPRX-2A* may regulate expression of these genes, thereby affecting salt tolerance. Future study will explore the mechanism by which *TaPRX-2A* exerts a regulatory function over other antioxidant-encoding genes.

Interestingly, we found that *TaPRX-2A* was localized in the nucleus with nuclear localization signals. Some reports showed that peroxidases were located in nucleus, such as *TaPRXs*, *AtGPX8*, GPX in mammals, *LjGpx1* [70,71,72,73,74]. It was reported that a barely peroxidase possess a putative nuclear localization signal, which located in the nucleus [75]. Previous studies have shown that ROS could cause DNA damage by activating endonuclease and damaging the important biological macromolecules (such as nucleic acids) [5,76,77]. In *Arabidopsis, AtGPX8* is localized in nucleus and can protect the nuclear DNA from ROS damage by maintaining cellular redox homeostasis [71]. On the basis of these, we propose possible mechanisms for this issue: one explanation is that *TaPRX-2A* is expressly conserved for inhibiting ROS-mediated damage to genomic DNA in the nucleus, and that other enzymes are responsible for scavenging ROS in or adjacent to organelles. Our second explanation is that *TaPRX-2A* is co-expressed with other ROS-scavenging enzymes, and its transcriptional up-regulation leads to up-regulation of enzymes that modulate ROS levels outside of the nucleus during salinity stress (Fig. 7).

TaPRX-2A enhanced the salt tolerance by the ABA-dependent pathway

In plants, ABA signaling pathway was a regulator to participate the abiotic stress response [78,79]. For example, dehydrin genes and thaumatin-like proteins (*TLP*) genes which are essential for abiotic stress tolerance may be induced by ABA during stress [80,81]. In *Arabidopsis*, ABA reportedly mediates transcriptional up-regulation of dehydration-responsive gene *RD22* [79]. Similar to *TaPRX-2A*, several class III PRXs are reported to mediate abiotic stress tolerance via the ABA signaling pathway [82]. For example, the expression of *AtPRX3* in *A. thaliana* is induced by both salt stress and exogenous ABA treatment [65]. Seven class III PRXs genes from *Tamarix Hispida* are controlled by ABA signaling pathway [83]. In our study, the expression of *TaPRX-2A* was highly up-regulated by both NaCl and exogenous ABA treatments (Fig. 3). Moreover, we observed that overexpression of *TaPRX-2A* in transgenic wheat led to transcriptional induction of stress-related genes *RD22, TLP4, ABAI, GLP4* and *GST2*2 under salt treatment (Fig. 7). Our work provided that *TaPRX-2A* enhanced salt tolerance of wheat through activating the downstream stress-related genes and ABA signaling pathway. Further study will explore the regulatory mechanisms by which *TaPRX-2A* exerts a regulatory function over stress-related genes.

Conclusions

In this study, we isolated and characterize the role of peroxidase gene *TaPRX-2A* in the wheat response to salt stress. Evolutionary analysis reveal that some exon fusion events and positive selection might have happened during *TaPRX-2A* evolution. Overexpression of *TaPRX-2A* enhanced salt tolerance in transgenic wheat plants by activation of ABA pathway and antioxidant enzymes, resulting in decreasing ROS accumulation and increasing osmotic metabolites. This work has strong application value for the cultivation of the salt-tolerant wheat varieties in the future, which is especially relevant given the anticipated hydrodynamics changes associated with ongoing climate change.

Abbreviations

WT, wild type; PRXs, peroxidases; SOD, superoxide dismutase; POD, peroxidase; CAT, catalase; ROS, reactive oxygen species; GPX, glutathione peroxidase; APX, ascorbate peroxidase; SA, salicylic acid; MeJA, methyljasmonic acid; IAA, indole-3-acetic acid; ABA, abscisic acid; RWC, relative water content; NBT, Nitroblue Tetrazolium; DAB, 3-diaminobenzidine; GFP, green fluorescent protein; qRT-PCR, quantitative real-time PCR; PEG6000, polyethylene glycol 6000.

Methods

Isolation and cloning of the *TaPRX-2A* gene and transformation

The leaves of harvest wheat cultivar “Sumai 3” were used to extract the total RNA by using TRIzol reagent (Transgen). cDNA was synthesized to amplify the *TaPRX-2A.* The full length cDNA sequence of *TaPRX-2A*

(Genbank No. AJ878510.1) was obtain from NCBI (https://www.ncbi.nlm.nih.gov/). The *TaPRX-2A* cDNA was ligated into the PC186 vector and then transformed into KN199 using particle gun mediated gene transformation [37].

Plant materials and abiotic treatments

Bread wheat (*T. aestivum* cultivar “KN199” and "Sumai 3") seedlings were sourced from our laboratory (State Key Laboratory of Crop Biology, College of Agronomy, Shandong Agricultural University). The *TaPRX-2A*-overexpressing transgenic wheat lines and wild type “KN199” were grown at 20°C-25°C with a photoperiod of 16 h/8 h. When the plants grew to a period of one leaf and one heart, the transgenic plants and “KN199” were treated with 200 mM NaCl treatment. In regard to salt treatment, the control and transgenic seedlings were cultured in 200 mM NaCl solution for 10 days.

Identification and classification of class III peroxidases in wheat, *Ae. tauschii*, and other plants

The genomes and proteomes of 12 plants including *S. moellendorffii*、*Z. mays*, *B. distachyon*, *T. aestivum, Ae. tauschii*, *T. dicoccoides, V. vinifera, T. urartu, O. sativa*, *A. thaliana*, *P. patens* and *C. reinhardtii*, were downloaded from Ensembl plants 42 (http://plants.ensembl.org/) and analyzed. To identify the PRXs, we scanned all the proteomes of 12 plants in batch mode by our own local server with Hmmer 3.1 (pfam profile PF00141.23, peroxidase.hmm, PRX domain). Then website pfam32.0 (http://pfam.xfam.org/) with an E value of 0.01 were performed. Typical PRXs with a PRX domain covering more than 50% alignment were retained and analyzed. Others covering less than 50% PRX domain alignment were considered as atypical PRXs and excluded in the following analysis. PRX alignment of truncated sequences in the PRX domain was performed by ClustalW v2.0 [38]. We used the software MEGA-CC 7.0 to construct the NJ phylogenetic tree in our local server [39]. The PRX subfamilies classification was performed by HMMER3.1, and the models were generated based on the maize PRX alignments [12].

The RNA-seq data of *P. patens* (SRR11434644, SRR11434645 and SRR11434646), *A. thaliana* (SRR11308184, SRR11308187 and SRR11308188), *V. vinifera* (SRR11249050, SRR11249059 and SRR11249060), *B. distachyon* (SRR10380965, SRR10380966, SRR10380967 and SRR10380968), *Ae. tauschii* (SRR9657462 and SRR9657463) and *T. dicoccoides* (SRR9657450 and SRR9657451) were downloaded from NCBI SRA transcriptome database (https://www.ncbi.nlm.nih.gov/sra/). The RNA-seq data of *T. aestivum* (ERR1201797, ERR1201798 and ERR1201799) were downloaded from EBI ArrayExpress (https://www.ebi.ac.uk/arrayexpress/). Mapping of sample reads to reference genome (Ensembl plants 42) was conducted by Hisat2 (version 2.2.0, https://daehwankimlab.github.io/hisat2/download/#version-hisat2-220). Conversion (sam to bam) and sort were performed by Samtools (version 1.10, https://github.com/samtools/samtools/releases/). The

transcripts were assembled by Stringtie (version 2.1.1, https://ccb.jhu.edu/software/stringtie/index.shtml).

Domain and intron–exon structure diagram of PRXs

We used our Perl and R scripts to generate the PRXs intron–exon structures and domain diagrams of these 12 plants based on the corresponding GFF file information from Ensembl Plants 42 (http://plants.ensembl.org/). The domain information of PRXs was batched from pfam 32.0 (http://pfam.xfam.org/).

Analysis of selective pressure

The truncated amino acid PRX domain sequences in *TaPRX-2A* and other 12 homologous PRXs were aligned by Clustal X2. Based on the information of pfam 32, the corresponding truncated cDNA of PRX domain was generated by our perl scripts. The codon alignment was generated by web server PAL2NAL [40]. The PAML 4.9 (CODEML) [41] and graphical interface PAMLX [42] were used to detect the selective pressure. Site-specific models M0 (one ratio), M1a (neutral), M2a (selection), M7 (beta) and M8 (beta & ω) were performed. Log likelihood (lnL) value of each model was calculated by CODEML. Comparison between models were checked by $2\Delta \text{lnL}=2(\text{lnL1}-\text{lnL0})$ obeying the $\chi 2$ distribution with the degrees of freedom (df). Ancestral sequences were inferred by CODEML (rst file of results) and MEGAX (using the ML method and JTT matrix-based model) [43].

Expression pattern of *TaPRX-2A* induced by different abiotic stress treatments

The wheat leaf tissues of three-leaf stage seedlings were harvested at 0, 6, 12, 24, 48 and 72 h after 20% (w/v) PEG 6000 treatment and 200 mM NaCl treatment. The wheat leaf tissues were harvested at 0, 2, 6, 12, 24, 48 and 72 h after 10 mM H_2O_2 treatment. We harvested the wheat leaf tissues at 0, 1, 3, 6, 12, 24 and 48 h after 2 mM salicylic acid (SA), 100 μM methyljasmonic acid (MeJA), 100 μM indole-3-acetic acid (IAA), and 100 mM abscisic acid (ABA) treatments. Total RNA of all harvested samples was extracted by using TRIzol reagent (Invitrogen). Synthesis of first-strand cDNA and qRT-PCR were performed by Roche LightCycler®480 (Roche, Germany). Wheat gene *18SrRNA* was used as an endogenous control. Relative mRNA expressions were calculated using the $2^{-\Delta\Delta CT}$ method. All qRT-PCR primers were supplied in Additional file 11: Table S5.

Subcellular localization of the *TaPRX-2A* protein

According to the ORF of the gene *TaPRX-2A*, we cloned this gene without stop codon, and then constructed it into pBIN*35S-eGFP* vector with the CaMV 35S promoter. Subsequently, the pBIN*35S-TaPRX-2A-eGFP* and pBIN*35S-eGFP* (control) were transformed into *Agrobacterium* EHA105. The *Agrobacterium* EHA105 was resuspended in the suspension (10 mM $MgCl_2$, 10 mM 4-morpholineethane -sulfonic acid hydrate (MES) (pH 5.6), 200 mM acetosyringone). The *Agrobacterium* suspension was adjusted about OD600 value 0.6, then injected into tobacco leaves and cultured for 3 days. The epidermal cells of the injected tobacco leaves were observed by confocal microscope. In addition, we also transformed the pBIN*35S-TaPRX-2A-eGFP* and pBIN*35S-eGFP* vector into onion epidermal cells by gene gun mediated transformation [44]. The transformed epidermal cells were cultured in darkness at 28℃ for 8-12 h, then observed by confocal microscope (Zeiss LSM880 Meta Confocal Microscope). NLSs (nuclear localization signals) sequences of *TaPRX-2A* were predicted by web server cNLS (http://nls-mapper.iab.keio.ac.jp/cgi-bin/NLS_Mapper_form.cgi) [45].

Measurements of physiological-biochemical parameters

We collected leaves of *TaPRX-2A*-overexpression and “KN199” plants at 10 days after salt treatment. We used the formula RWC = (FW-DW) / (TW-DW) × 100% (relative water content (RWC), fresh weight (FW), turgid fresh weight (TW), dry weight (DW)) to measure the leaf RWC [46]. MDA content was measured by thiobarbituric acid method [47]. Proline content was measured by ninhydrin reaction method [48]. Soluble total sugars were determined by the anthrone method [49]. We used nitroblue tetrazolium (NBT) and 3, 3’-diaminobenzidine (DAB) to visualize O_2^- and H_2O_2. The H_2O_2 and O_2^- levels were measured by methods [50, 51]. The SOD, CAT and PRX activity were detected using methods [52, 53, 54].

Declarations

Ethics approval and consent to participate

The wheat materials (cultivar “KN199” and "Sumai 3") used in this study were obtained from the State Key Laboratory of Crop Biology, College of Agronomy, Shandong Agricultural University, Tai'an, Shandong, PR China. They are publicly available for non-commercial purposes.

Consent for publication

Not applicable.

Availability of data and materials

The genomes and proteomes of investigated plants are available in Ensembl Plants (http://plants.ensembl.org/). The accession numbers of investigated plants are *T. aestivum* (IWGSC), *Ae. tauschii* (Aet_v4.0), *A. thaliana* (TAIR10), *B. distachyon* (v3.0), *C. reinhardtii* (v5.5), *O. sativa* (IRGSP-1.0), *P. patens* (Phypa_V3), *S. moellendorffii* (v1.0), *T. dicoccoides* (WEWSeq_v.1.0), *T. urartu* (ASM34745v1), *V. vinifera* (12X), and *Z. mays* (B73_RefGen_v4). The nucleotid and amino acid sequence of T*aPRX-2A* is available at NCBI with accession number AJ878510.1 (https://www.ncbi.nlm.nih.gov/). The accession numbers of using RNA-seq data from NCBI SRA and EBI ArrayExpress were shown in Method section. The identification and exon-intron structures of PRXs in investigated plants are provided in supplementary files.

Competing interests

The authors declare that they have no competing interests.

Funding

This work was supported by the National Natural Science Foundation of China (3315203911 and 31471488), the Transgenic Special Item of China (2016ZX08002003-002 and 2016ZX08009-003), the National Key Research and Development Program of China (2016YFD0100602). The funding body had no role in the design of the study and collection, analysis, and interpretation of data and in writing the manuscript.

Authors' contributions

PSS, HWW and LRK conceived and designed the experiments; PSS performed most of the experiments; JY performed the identification and evolution analysis of *TaPRX-2A*, and revised the manuscript; LW, JXZ and WL performed the subcellular localization and plant transformation; AFL contributed plant materials; PSS wrote and revised the manuscript. All authors have read and approved the final manuscript.

Acknowledgements

We thank to Prof. Shumei Zhou (Shandong Agricultural University, China) for help in the measurement of physiological data.

References

1. Mahajan S, Tuteja N. Cold, salinity and drought stresses: an overview. Arch Biochem Biophys. 2005;444:139-158.
2. Shinozaki K, Yamaguchi-Shinozaki K. Molecular responses to dehydration and low temperature: differences and cross-talk between two stress signaling pathways. Curr. Opin. Plant Biol. 2000;3:217-223.
3. Campo S, Baldrich P, Messeguer J, Lalanne E, Coca M, San Segundo B. Overexpression of a calcium-dependent protein kinase confers salt and drought tolerance in rice by preventing membrane lipid peroxidation. Plant Physiol. 2014;165:688-704.
4. Abdel Latef AA, Kordrostam M, Zakir A, Zaki H, Saleh OM. Eustress with H_2O_2 facilitates plant growth by improving tolerance to salt stress in two wheat cultivars. Plants. 2019a; 8(9):303.
5. McCord JM. The evolution of free radicals and oxidative stress. Am J Med. 2000;108: 652–659.
6. Roxas VP, Lodhi SA, Garrett DK, Mahan JR, Allen RD. Stress tolerance in transgenic tobacco seedlings that overexpress glutathione S-transferase/glutathione peroxidase. Plant Cell Physiol. 2000;41:1229-1234.
7. Zhai CZ, Zhao L, Yin LJ, Chen M, Wang QY, Li LC, Ma YZ. Two wheat glutathione peroxidase genes whose products are located in chloroplasts improve salt and H_2O_2 tolerances in *Arabidopsis*. PloS one. 2013;8: e73989.
8. Mittler R. Oxidative stress, antioxidants and stress tolerance. Trends Plant Sci. 2002;7:405-410.
9. Abdel Latef AA, Mostofa MG, Rahman MM, Abdel Farid IB, Tran LSP. Extracts from yeast and carrot roots enhance maize performance under seawater-induced salt stress by altering physio-biochemical characteristics of stressed plants. J Plant Growth Regul. 2019b; 38:966-979.
10. Abdel Latef AA, Abu Alhmad MF, Kordrostami M, Abo-Baker AE, Zakir A. Inoculation with *Azospirillum lipoferum* or *Azotobacter chroococcum* reinforces maize growth by improving physiological activities under saline conditions. J Plant Growth Regul. 2020. https://doi.org/10.1007/s00344-020-10065-9.
11. Mu Y, Lian FM, Teng YB, Ao J, Jiang YL, He YX, Chen, X. The N-terminal β-sheet of peroxiredoxin 4 in the large yellow croaker *Pseudosciaena crocea* is involved in its biological functions. PloS one. 2013;8:e57061.
12. Wang Y, Wang Q, Zhao Y, Han G, Zhu S. Systematic analysis of maize class III peroxidase gene family reveals a conserved subfamily involved in abiotic stress response. Gene. 2015;566:95-108.
13. Hiraga S, Sasaki K, Ito H, Ohashi Y, Matsui H. A large family of class III plant peroxidases. Plant Cell Physiol. 2001;42:462–468.
14. Welinder KG. Superfamily of plant, fungal and bacterial peroxidases, Curr. Opin. Struct. Biol. 1992; 2:388-393.
15. Taurog A. Molecular evolution of thyroid peroxidase. Biochimie, 1999;81:557-562.
16. Cosio C, Dunand C. Specific functions of individual class III peroxidase genes. J. Exp. Bot. 2009;60:391–408.

17. Shigeoka S, Ishikawa T, Tamoi M, Miyagawa Y, Takeda, T, Yabuta Y, Yoshimura K. Regulation and function of ascorbate peroxidase isoenzymes. J. Exp. Bot. 2002;53:1305–1319.
18. Erman JE, Vitello LB. Yeast cytochrome c peroxidase: mechanistic studies via protein engineering. Biochimica Et Biophysica Acta (BBA)-Protein Structure and Molecular Enzymology. 2002;1597:193–220.
19. Martinez AT, Speranza M, Ruiz-Duenas FJ, Ferreira P, Camarero S, Guillen F, Martinez MJ, Gutierrez A, del Río JC. Biodegradation of lignocellulosics: microbial, chemical, and enzymatic aspects of the fungal attack of lignin. Int. Microbiol. 2005;8:195–204.
20. Almagro L, Gómez LV, Belchi-Navarro S, Bru R, Ros Barceló A, Pedreno MA. Class III peroxidases in plant defence reactions. J. Exp. Bot. 2009;60:377-390.
21. Csiszár J, Gallé Á, Horváth E, Dancsó P, Gombos M, Váry Z, Tari I. Different peroxidase activities and expression of abiotic stress-related peroxidases in apical root segments of wheat genotypes with different drought stress tolerance under osmotic stress. Plant Physiol. Biochem. 2012;52:119-129.
22. Passardi F, Longet D, Penel C, Dunand C. The class III peroxidase multigenic family in rice and its evolution in land plants. Phytochemistry. 2004;65:1879-1893.
23. Welinder KG, Justesen AF, Kjaersgard IV, Jensen RB, Rasmussen SK, Jespersen HM, Duroux L. Structural diversity and transcription of class III peroxidases from *Arabidopsis thaliana*. European Journal of Biochemistry. 2002;269:6063–6081
24. Ren LL, Liu YJ, Liu HJ, Qian TT, Qi LW, Wang XR, Zeng QY. Subcellular relocalization and positive selection play key roles in the retention of duplicate genes of *Populus* class III peroxidase family. Plant Cell. 2014;26:2404–2419.
25. De GL. Class III peroxidases and ascorbate metabolism in plants. Phytochem. Rev. 2004;3:195-205.
26. Herrero J, Fernández-Pérez F, Yebra T, Novo-Uzal E, Pomar F, Pedreño MÁ, Cuello J, Guéra A, Esteban-Carrasco A, Zapata JM. Bioinformatic and functional characterization of the basic peroxidase 72 from *Arabidopsis thaliana* involved in lignin biosynthesis. Planta. 2013; 237:1599–1612.
27. Cheong YH, Chang HS, Gupta R, Wang X, Zhu T, Luan S. Transcriptional profiling reveals novel interactions between wounding, pathogen, abiotic stress, and hormonal responses in *Arabidopsis*. Plant Physiol. 2002; 129:661–677.
28. Chassot N, Nawrath C, Métraux JP. Cuticular defects lead to full immunity to a major plant pathogen. Plant J. 2007;49:972-980.
29. Mei WQ, Qin YM, Song WQ, Li J, Zhu YX. Cotton *GhPOX1* encoding plant class III peroxidase may be responsible for the high level of reactive oxygen species production that is related to cotton fiber elongation. J. Genet. Genomics. 2009;36:141–150.
30. Simonetti E, Veronico P, Melillo MT, Delibes Á, Andrés MF, López-Braña I. Analysis of class III peroxidase genes expressed in roots of resistant and susceptible wheat lines infected by *Heterodera avenae*. Mol. Plant-Microbe Interact. 2009;22:1081-1092.
31. Hiraga T, Ichinose C, Onogi T, Niki H, Yamazoe M. Bidirectional migration of SeqA-bound hemimethylated DNA clusters and pairing of oriC copies in *Escherichia coli*. Genes Cells.

2000;5:327–341.

32. Miao Y, Lv D, Wang P, Wang XC, Chen J, Miao C, Song CP. An *Arabidopsis* glutathione peroxidase functions as both a redox transducer and a scavenger in abscisic acid and drought stress responses. Plant Cell. 2006;18:2749-2766.
33. Zhou Y, Hu LF, Ye SF, Jiang LW, Liu SQ. Genome-wide identification of glutathione peroxidase (GPX) gene family and their response to abiotic stress in *Cucumber*. 3 Biotech. 2018;8:159.
34. Sečenji M, Lendvai Á, Miskolczi P, Kocsy G, Gallé Á, Szűcs A, Hoffmann B, Sa´rva´ri E, Schweizer P, Stein N, Dudits D, Gyorgyey J. Differences in root functions during long-term drought adaptation: comparison of active gene sets of two wheat genotypes. Plant Biol. 2010;12:871-882.
35. Dong W, Wang MC, Xu F, Quan TY, Peng KQ, Xiao LT, Xia GM. Wheat oxophytodienoate reductase gene *TaOPR1* confers salinity tolerance via enhancement of abscisic acid signaling and reactive oxygen species scavenging. Plant Physiol. 2013;161:1217-1228.
36. Zhang M, Lv DW, Ge P, Bian YW, Chen GX, Zhu GR, Li XH, Yan YM. Phosphoproteome analysis reveals new drought response and defense mechanisms of seedling leaves in bread wheat (*Triticum aestivum* L.). J. Proteomics. 2014;109:290-308.
37. Yao Q, Cong L, Chang JL, Li KX, Yang GX, He GY. Low copy number gene transfer and stable expression in a commercial wheat cultivar via particle bombardment. J. Exp. Bot. 2006;57:3737-3746.
38. Larkin MA, Blackshields G, Brown NP, Chenna R, McGettigan PA, McWilliam H, Valentin F, Wallace IM, Wilm A, Lopez R. Clustal W and Clustal X version 2.0. Bioinformatics. 2007;23:2947-2948.
39. Kumar S, Stecher G, Tamura K. MEGA7: Molecular evolutionary genetics analysis version 7.0 for bigger datasets. Mol. Biol. Evol. 2016;33:1870-1874.
40. Suyama M, Torrents D, Bork P. PAL2NAL: robust conversion of protein sequence alignments into the corresponding codon alignments. Nucleic Acids Res. 2006;34:609-612.

41.Yang Z. PAML 4: a program package for phylogenetic analysis by maximum likelihood. Mol. Biol. Evol. 2007; 24:1586-1591.

42. Xu B, Zhang ZH. pamlX: a graphical user interface for PAML. Mol. Biol. Evol. 2013; 30:2723-2724.
43. Kumar S, Stecher G, Li M, Knyaz C, Tamura K. MEGA X: Molecular evolutionary genetics analysis across computing platforms. Mol. Biol. Evol. 2018;35:1547-1549.
44. Das P, Ito T, Wellmer F, Vernoux T, Dedieu A, Traas J, Meyerowitz EM. Floral stem cell termination involves the direct regulation of agamous by perianthia. Development. 2009;136:1605-1611.
45. Kosugi S, Hasebe M, Tomita M, and Yanagawa H. Systematic identification of yeast cell cycle-dependent nucleocytoplasmic shuttling proteins by prediction of composite motifs. Proc. Natl. Acad. Sci. 2009;106: 10171-10176.
46. Zhou SM, Sun XD, Yin SH, Kong XZ, Zhou S, Xu Y, Wang W. The role of the F-box gene *TaFBA1* from wheat (*Triticum aestivum* L.) in drought tolerance. Plant Physiol. Biochem. 2014;84:213-223.

47. Heath R, Packer L. Photoperoxidation in isolated chloroplasts: I. Kinetics and stoichiometry of fatty acid peroxidation. Arch Biochem Biophys. 1968;125:189–198
48. Bates LS, Waldren PR, Teare ID. Rapid determination of free proline for water-stress studies. Plant Soil. 1973;39: 205–207.
49. Spiro RG. Analysis of sugars found in glycoprotein. Method in enzymology, 1966;8:3-26.
50. Gay C, Collins J, Gebicki JM. Hydroperoxide assay with the ferric-xylenol orange complex. Anal. Biochem. 1999;273:149-155.
51. Tian F, Gong J, Zhang J, Zhang M, Wang G, Li A, Wang W. Enhanced stability of thylakoid membrane proteins and antioxidant competence contribute to drought stress resistance in the *tasg1* wheat stay-green mutant. J. Exp. Bot. 2013;64:1509-1520.
52. Dhindsa RA, Plumb-Dhindsa P, Thorpe TA. Leaf senescence: correlated with increased permeability and lipid peroxidation, and decreased levels of superoxide dismutase and catalase. J. Exp. Bot. 1981; 126:93–101.
53. Aebi H. Catalase in vitro. Methods Enzymol. 1984; 105: 121–126.
54. Chance B, Maehly A. [136] assay of catalases and peroxidases. Methods Enzymol. 1955;2:764-775.
55. Hu LX, Li HY, Pang HC, Fu JM. Responses of antioxidant gene, protein and enzymes to salinity stress in two genotypes of perennial ryegrass (*Lolium perenne*) differing in salt tolerance. J. Plant Physiol. 2012;169 :146-156.
56. Mittler P, Vanderauwera S, Suzuki N, Miller G, Tognetti VB, Vandepoele K, Gollery M, Shulaev V, Breusegem FV. ROS signaling: the new wave? Trends Plant Sci. 2011;16:300-309.
57. You J, Chan ZL. ROS regulation during abiotic stress responses in crop plants. Front. Plant Sci. 2015;6:1092.
58. Long M, Langley C. Natural selection and the origin of jingwei, a chimeric processed functional gene in *Drosophila*. Science. 1993; 260:91–95.
59. Long MY, Deutsch M, Wang W, Betrán E, Brunet FG, Zhang JM. Origin of new genes: evidence from experimental and computational analyses. Genetica. 2003;118:171-182.
60. Zhang Y, Wu Y, Liu Y, Han B. Computational identifcation of 69 retroposons in *Arabidopsis*. Plant Physiol. 2005;138: 935–948.
61. Wang W, Zheng HK, Fan CZ, Li J, Shi JJ, Cai ZQ, Zhang GJ, Liu DY, Zhang JG, Vang SR, Lu ZK, Wong G, Long MY, Wang J. High rate of chimeric gene origination by retroposition in plant genomes. The Plant Cell. 2006; 18:1791–1802.
62. Zhou YL, Zhang CJ. Evolutionary patterns of chimeric retrogenes in *Oryza* species. Sci Rep. 2019; 9:17733.
63. Maria K, Yogeshwar VD, Neelam G, Madhu T, Iffat ZA, Mehar HA, Debasis C. *Oryza sativa* class III peroxidase (*Osprx38*) overexpression in *Arabidopsis thaliana* reduces arsenic accumulation due to apoplastic lignification. J. Hazard. Mater. 2019;362:383-393.

64. Wu YS, Yang ZL, How, JY. Xu HN, Chen LM, Li KZ. Overexpression of a peroxidase gene (*AtPrx64*) of *Arabidopsis thaliana* in tobacco improves plant's tolerance to aluminum stress. Plant Mol Biol. 2017; 95:157–168.
65. Llorente F, Lopez-Cobollo RM, Catala R, Martinez-Zapater JM, Salinas J. A novel cold-inducible gene from *Arabidopsis, RCI3*, encodes a peroxidase that constitutes a component for stress tolerance. Plant J. 2002; 32:13–24.
66. Kumar S, Jaggi M, Sinha AK. Ectopic overexpression of vacuolar and apoplastic *Catharanthus roseus* peroxidases confers differential tolerance to salt and dehydration stress in transgenic tobacco. Protoplasma. 2012; 249: 423–432.
67. Dat J, Vandenabeele S, Vranová E, Van MM, Inzé D, Van BF. Dual action of the active oxygen species during plant stress responses. Cell. Mol. Life Sci. 2000;57:779-795.
68. Baxter A, Mittler R, Suzuki N N. ROS as key players in plant stress signaling. J. Exp. Bot. 2013;65:1229-1240.
69. Gill SS, Tuteja N. Reactive oxygen species and antioxidant machinery in abiotic stress tolerance in crop plants. Plant Physiol. Biochem. 2010;48:909-930.

70.Yan J, Su PS, Li W.Xiao GL, Zhao Y, Ma X, Wang HW, Nevo E, Kong LR. Genome-wide and evolutionary analysis of the class III peroxidase gene family in wheat and *Aegilops tauschii* reveals that some members are involved in stress responses. BMC Genomics. 2019; 20:666.

71. Ahmed G, Tomoya O, Takanori M, Kazuya Y, Masahiro T, Shigeru S. The involvement of *Arabidopsis* glutathione peroxidase 8 in the suppression of oxidative damage in the nucleus and cytosol. Plant Cell Physiol. 2012; 53:1596–1606.
72. Del Maestro R, McDonald W. Subcellular localization of superoxide dismutases, glutathione peroxidase and catalase in developing rat cerebral cortex. Mech. Ageing Dev. 1989;48: 15–31.
73. Rogers LK, Gupta S, Welty SE, Hansen TN, Smith CV. Nuclear and nucleolar glutathione reductase, peroxidase, and transferase activities in livers of male and female Fischer-344 rats. Toxicol. Sci. 2002;69: 279–285.
74. Matamoros MA, Saiz A, Peñuelas M, Bustos-Sanmamed P, Mulet JM, Barja MV, Rouhier N, Moore M, James EK, Dietz KJ, Becana M. Function of glutathione peroxidases in legume root nodules. J. Exp. Bot. 2015; 66:2979–2990.
75. Stacy RA, Nordeng TW, Culianez-Macia FA, Aalen RB. The dormancy-related peroxiredoxin anti-oxidant, PER1, is localized to the nucleus of barley embryo and aleurone cells. J. Plant. 1999; 19:1–8.
76. Hagar H, Ueda N, Shah SV. Role of reactive oxygen metabolites in DNA damage and cell death in chemical hypoxic injury to LLC-PK1 cells. Amer. J. Physiol. 1996;271: 209–215.
77. Chen SX, Schopfer P. Hydroxyl radical production in physiological reactions: A novel function of peroxidase. Eur. J.Biochem. 1999;260: 726–735.
78. Chinnusamy V, Gong Z, Zhu JK. Abscisic acid-mediated epigenetic processes in plant development and stress responses. J. Integr. Plant Biol. 2008;50:1187-1195.

79. Shinozaki K, Yamaguchi-Shinozaki K, Seki M. Regulatory network of gene expression in the drought and cold stress responses. Curr. Opin. Plant Biol. 2003;6:410-417.
80. Seo PJ, Park CM. MYB96-mediated abscisic acid signals induce pathogen resistance response by promoting salicylic acid biosynthesis in *Arabidopsis*. New Phytol. 2016;186:471-483.
81. Jung YC, Lee HJ, Yum SS, Soh WY, Cho DY, Auh CK, Lee TK, Soh HC, Kim YS, Lee SC. Drought-inducible-but ABA-independent-thaumatin-like protein from carrot (*Daucus carota L.*). Plant Cell Rep. 2005;24:366-373.
82. Roberts E, Kolattukudy PE. Molecular cloning, nucleotide sequence, and abscisic acid induction of a suberization-associated highly anionic peroxidase. Mol. Gen. Genom. 1989;217: 223–232.
83. Gao CQ, Wang YC, Liu GF, Wang C, Jiang J, Yang CP. Cloning of ten peroxidase (POD) Genes from *Tamarix Hispida* and characterization of their responses to abiotic stress. Plant Mol Biol Rep. 2010; 28: 77.

Additional File Information

Additional file 1: Table S1. The number of class III peroxidase gene family in 12 plants.

Additional file 2: Table S2. Subfamily classification of class III peroxidases in the investigated plant genomes.

Additional file 3: Table S3. List of atypical class III peroxidase in investigated plant genomes.

Additional file 4: Figure S1. Class III peroxidase phylogenetic tree. (a) Subfamily VI of class III peroxidases; (b) All subfamilies.

Additional file 5: Figure S2. Domain and exon-intron structure diagrams of class III peroxidase in *A. thaliana, V. vinifera, T. aestivum, P. patens, T. dicoccoides, T. urartu, Ae. tauschii, B. distachyon, C. reinhardtii, Z. mays, O. sativa* and *S. moellendorffii*. Filled boxes: red represents the PRX domain; white boxes represent the other exon regions; black boxes represent the untranslated regions (UTRs); lines represent the PRX introns; numbers 0, 1, and 2 represent the exon phases. The long introns are shortened by "//".

Additional file 6: Table S4. The cDNA-level evidence performing by RNA-seq data from seven plants.

Additional file 7: Figure S3. Positively selected sites and inferred ancestral sequences. (a) by using M2a model of PAML. (b) by using M8 model of PAML. (c) by using MEGAX. Inferred positively selected sites were circled by red boxes in the alignment of 13 PRXs and 11 inferred ancestral sequences.

Additional file 8: Figure S4. Localization of *TaPRX-2A* was mainly in nucleus. (a) Vector construction diagrams of *pBIN35S:eGFP* and *pBIN35S:TaPRX-2A:eGFP*. (b_1–d_2) Subcellular localization of the *pBIN35S:TaPRX-2A:eGFP* fusion protein and *pBIN35S:eGFP* protein in tobacco epidermal cells. (b_3–d_4) Subcellular localization of the *pBIN35S:TaPRX-2A:eGFP* fusion protein and *pBIN35S:eGFP* protein in

onion epidermal cells (b_1-b_4) Green fluorescent images; (c_1-c_4) Merged images of bright, green fluorescence; (d_1-d_4) Bright field images. Bars, 20 μm.

Additional file 9: Figure S5. The prediction of nuclear localization signals in *TaPRX-2A*.

Additional file 10: Figure S6. The expression profile and peroxidase activity measurement. (a) Expression analysis of *TaPRX-2A* in transgenic lines and WT by using *TaPRX-2A* gene. (b) The measurement of peroxidase activity in *TaPRX-2A* transgenic lines and WT. The gene *18SrRNA* was as an endogenous control. The gene relative expression was calculated by the cycle threshold (Ct) values using formula $2^{-\Delta\Delta CT}$. The data are means ± SD calculated from three technical replicates. Asterisks, * and **, above each column indicate significant difference compared with WT plants (*P <0.05; **P < 0.01).

Additional file 11: Table S5. Primers used for analysis.

Table

Table 1. Detection of positive selection of *TaPRX-2A* and other 12 homologous PRX genes in plants.

Models	np	Estimates of parameters	lnL	LRT pairs	df	2Δ lnL	P
M0: one ratio	1	ω= 0.12224	-5255.0007	M0 /M2	3	249.899394	<0.005
M1a: neutral	2	p_0= 0.74332, (p_1= 0.25668), ω_0= 0.06658, (ω_1= 1.00)	-5164.268639				
M2a: selection	4	p_0= 0.41411, p_1= 0.29296, (p_2= 0.29293), ω_0= 0.02081, (ω_1= 1.00), ω_2= 0.14800	-5130.051003	M1/M2	2	68.435272	<0.005
M7: beta	2	p= 0.53605, q= 2.52403	-5119.765697	M7/M8	2	7.47398	<0.025
M8: beta and ω	4	p_0= 0.66950, (p_1= 0.33050), P= 0.29052, q= 0.92947, ω= 0.09129	-5116.028707				

Abbreviation, np: number of free parameters; lnL: log likelihood; LRT: likelihood ratio test; df: degrees of freedom; 2Δ lnL: twice the log-likelihood difference of the models compared.

Figures

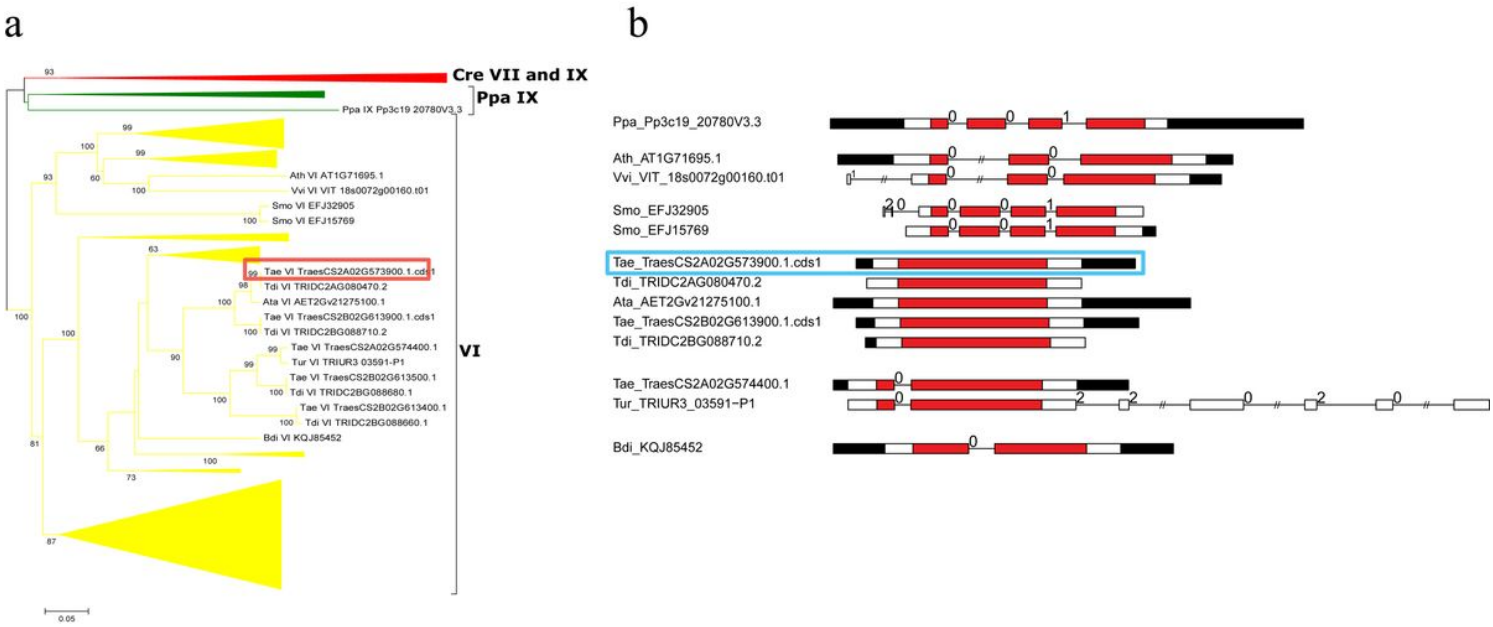

Figure 1

Phylogenetic tree and gene structures of TaPRX-2A and related PRXs in wheat, Ae. Tauschii, and other plants. (a) The diagram indicates the neighbor-joining tree. The amino acid sequences of the PRX domain were used to construct the neighbor-joining tree by using a software MEGA-CC 7.0 with the p-distance model. Most sequences belong to subfamily VI of class III peroxidases, and some branches are compressed. Detailed information is showed in Additional file 4: Figure S1. (b) The diagram indicated the exon-intron structures of some PRXs. Filled boxes: red boxes represent the PRX domain; white boxes represent the other exon regions; black boxes represent the untranslated regions (UTRs); lines represent the PRX introns; numbers 0, 1, and 2 represent the exon phases. The long introns are shortened by "//". Our investigated PRX (TraesCS2A02G573900.1.cds1) in T. aestivum was circled by a red or cyan box.

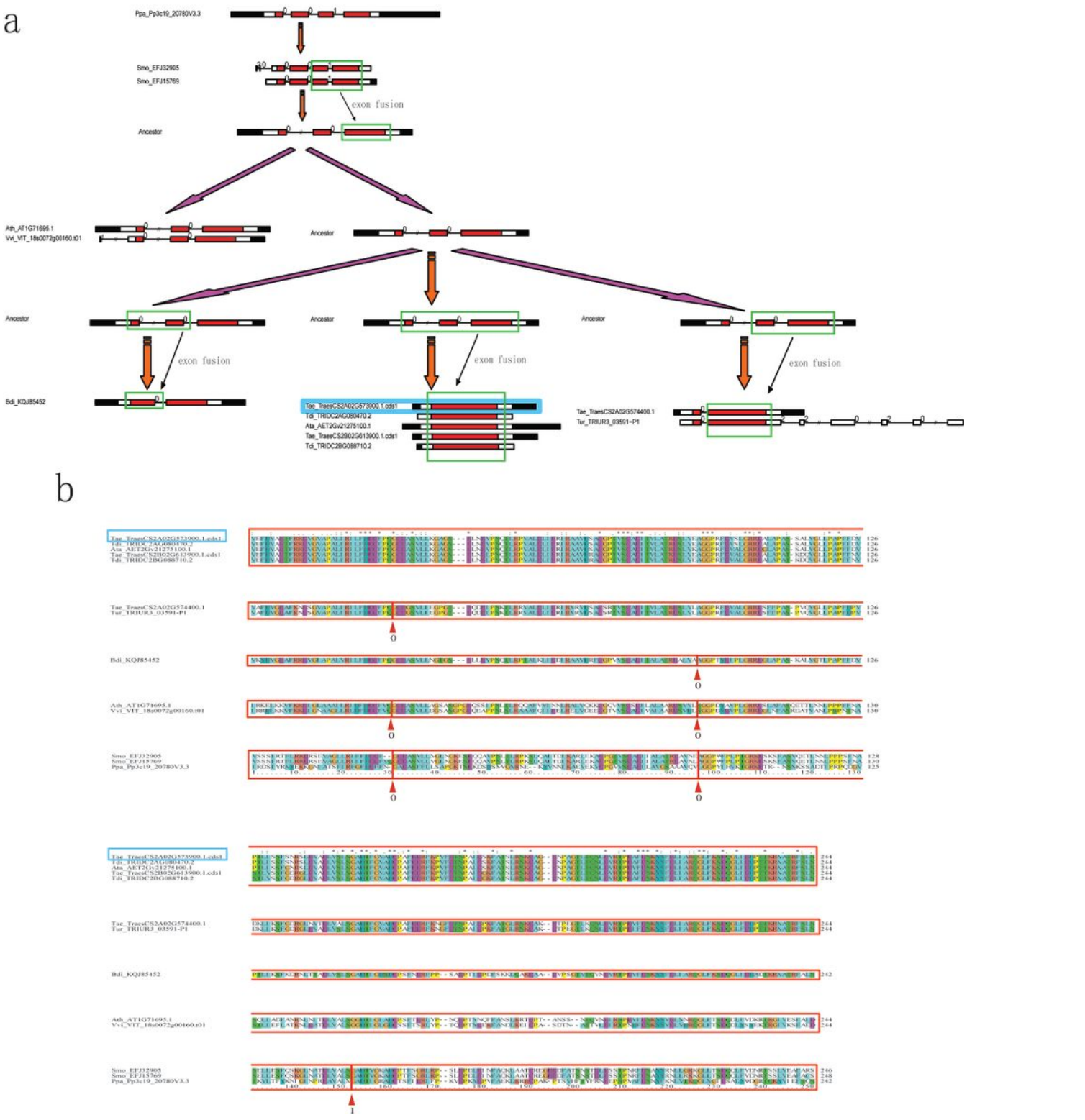

Figure 2

The evolutionary model of some subfamily VI PRXs including TaPRX-2A. (a) The exon fusions of some subfamily VI PRXs in evolution. (b) The alignment of some subfamily VI PRXs. The exon phases were circled by red boxes and arrows. Our investigated PRX (TraesCS2A02G573900.1.cds1) in T. aestivum was circled by cyan box.

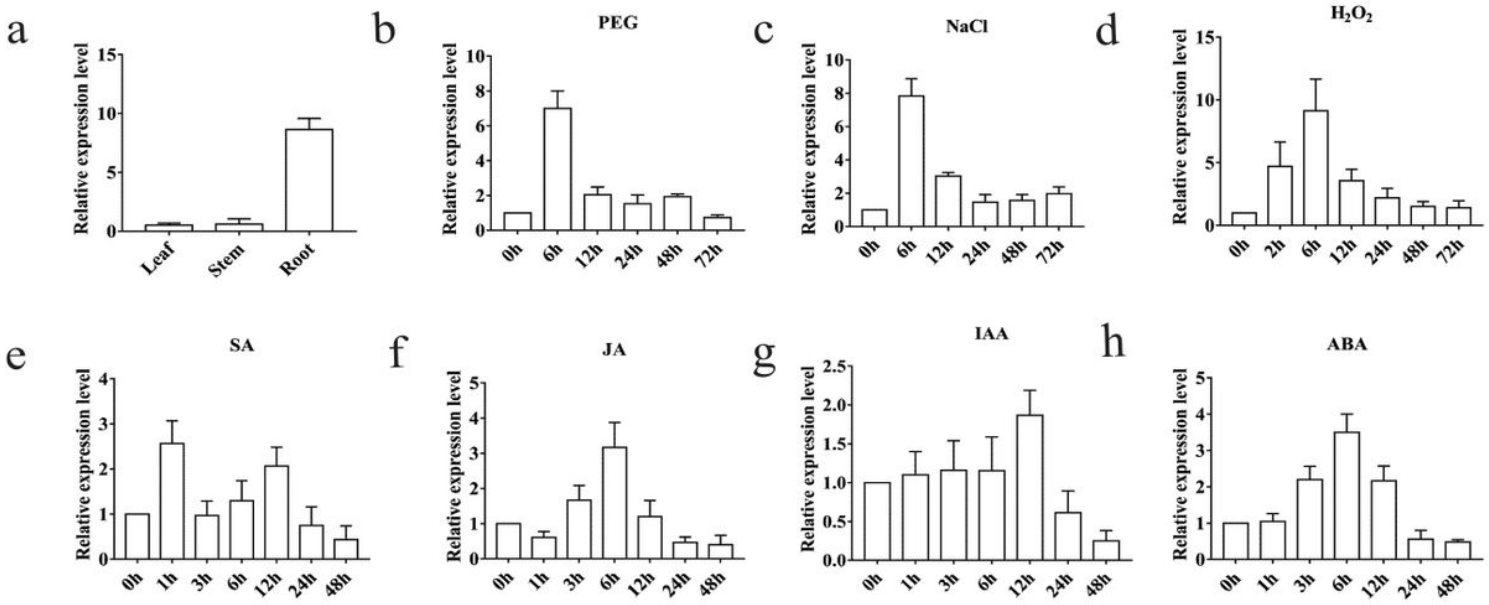

Figure 3

The transcript analysis of TaPRX-2A. (a) The TaPRX-2A expression levels in the leaves, roots, and stems. The TaPRX-2A expression was performed under different stress treatments, 20% (w/v) PEG 6000 (b), 200 mM NaCl (c), 10 mM H2O2 (d), 2 mM salicylic acid (SA) (e), 100 μM methyljasmonic acid (MeJA) (f), 100 μM indole-3-acetic acid (IAA) (g), and 100 mM abscisic acid (ABA) (h). The gene 18SrRNA was as an endogenous control. The gene relative expression was calculated by the cycle threshold (Ct) values using formula 2−ΔΔCT. The data are means ± SD calculated from three technical replicates.

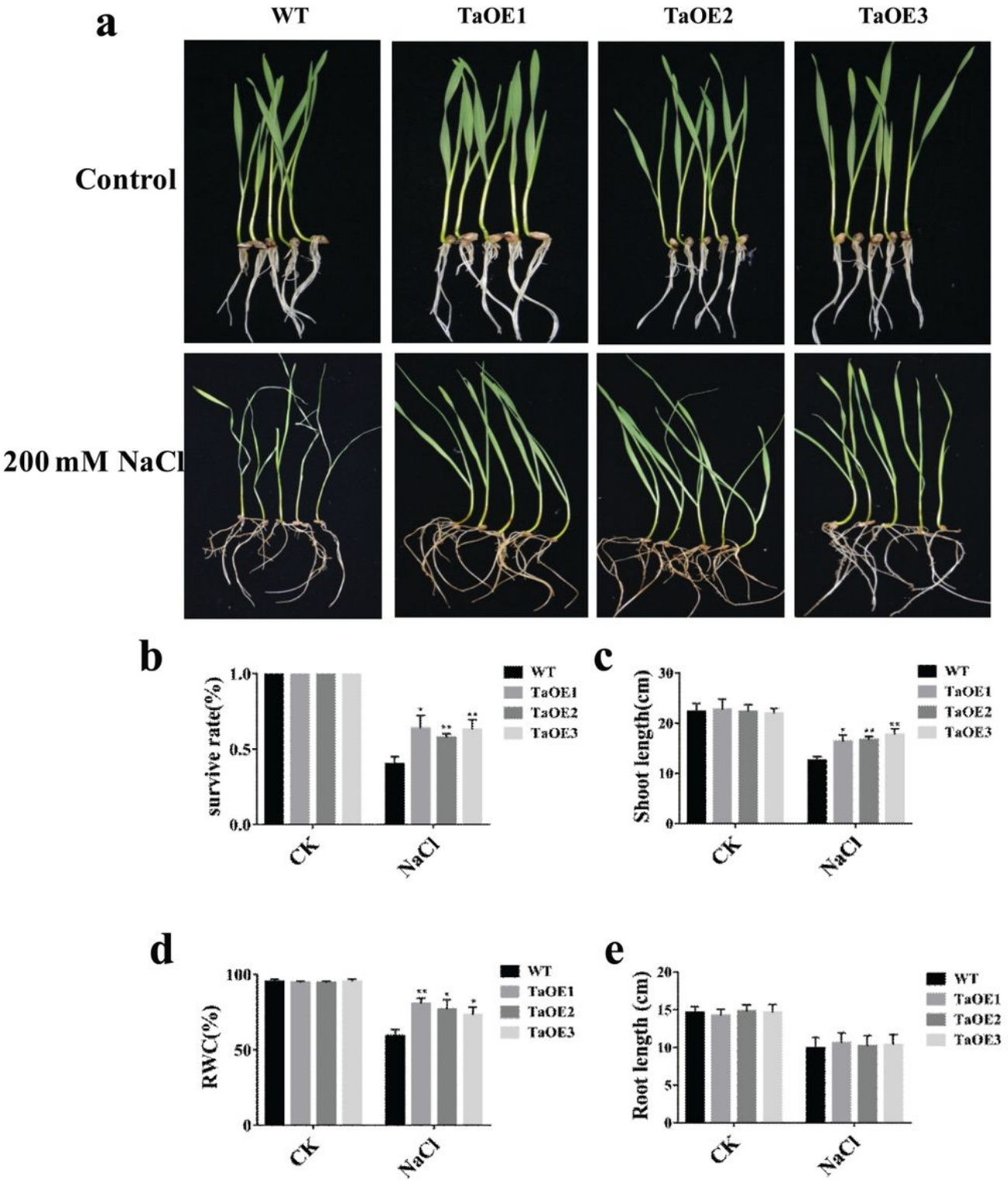

Figure 4

TaPRX-2A enhanced the salt tolerance of wheat. (a) Tolerance responses of the TaPRX-2A-overexpressing lines and wild type wheat (the cultivar “KN199”) to salt stress. (b) The survival rates. (c) The shoot length and (d) the root length of TaPRX-2A-overexpressing and WT plants. (e) The relative water content of TaPRX-2A-overexpressing and WT plants. The data are means ± SD calculated from three technical

replicates. Asterisks, * and **, above each column indicate significant difference compared with WT plants (*P <0.05; **P < 0.01).

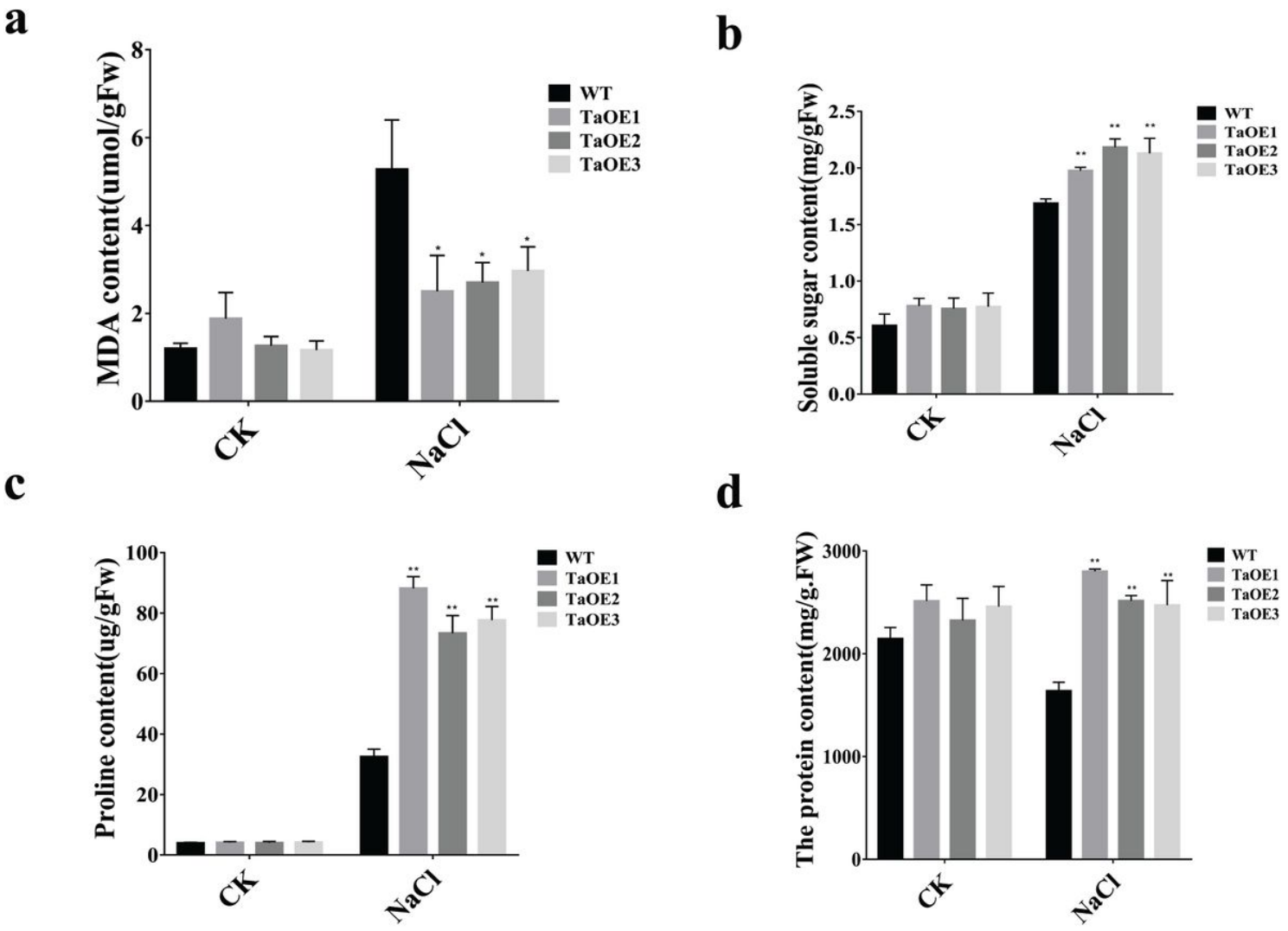

Figure 5

Physiological-biochemical indices between TaPRX-2A-overexpressing transgenic lines and WT plants. (a) MDA content. (b) Soluble sugar content. (c) Proline content. (d) The soluble protein content. The data are means ± SD calculated from three technical replicates. Asterisks, * and **, above each column indicate significant difference compared with WT plants (*P <0.05; **P < 0.01).

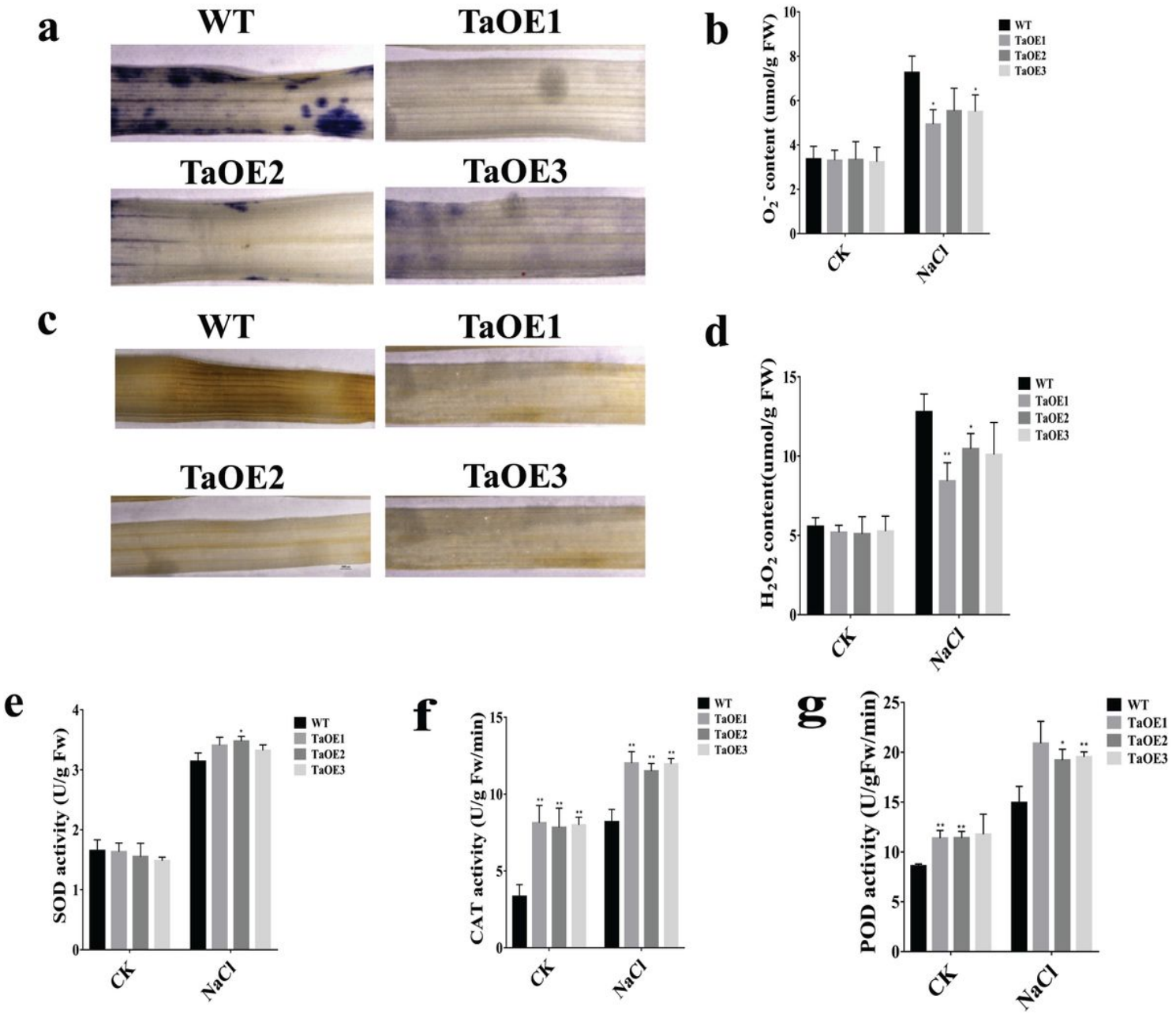

Figure 6

TaPRX-2A confers ROS-scavenging capacity by improving antioxidant enzymes activities. (a) Tissue localization of O2- accumulation. (b) O2- content. (c) Tissue localization of H2O2 generation. (d) H2O2 content. (e) SOD activity. (f) CAT activity. (g) POD activity. The data are means ± SD calculated from three technical replicates. Asterisks, * and **, above each column indicate significant difference compared with WT plants (*P <0.05; **P < 0.01).

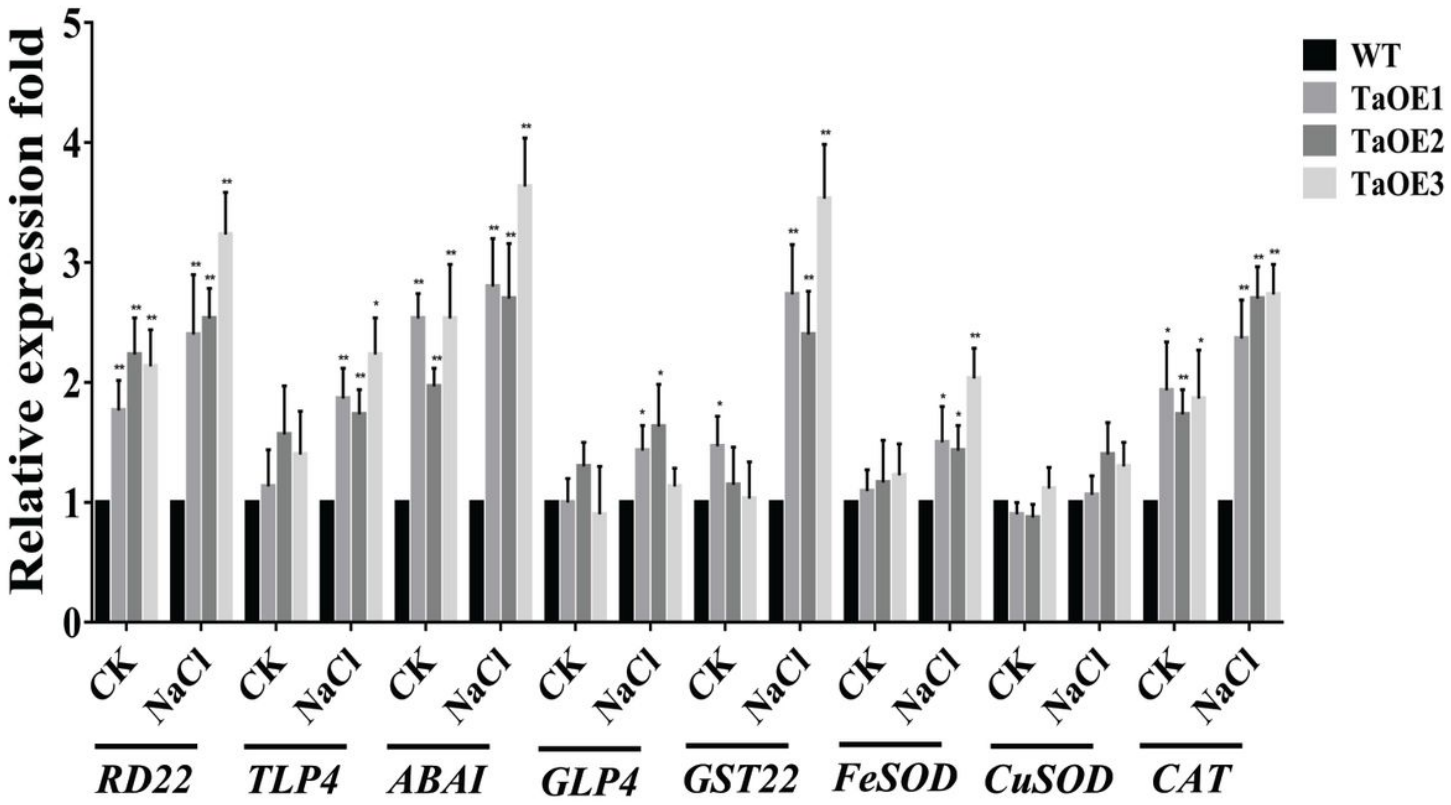

Figure 7

Analysis of transcript profile of some stress-related genes. The stress-related genes expression level in TaPRX-2A-overexpressing transgenic lines and WT plants under salt stress by qRT-PCR. The gene 18SrRNA was as an endogenous control. Each treatment had three independent biological repeats. The gene relative expression was calculated by the cycle threshold (Ct) values using formula $2-\Delta\Delta CT$. The data are means ± SD calculated from three technical replicates. Asterisks, * and **, above each column indicate significant difference compared with WT plants (*P <0.05; **P < 0.01).

Supplementary Files

This is a list of supplementary files associated with this preprint. Click to download.

- FigureS6.jpg
- FigureS3.pdf
- FigureS2.pdf
- FigureS1.pdf
- FigureS4.jpg
- FigureS5.pdf
- TableS5.xls

- TableS1.xls
- TableS4.xls
- TableS2.xls
- TableS3.xls